Electronic Supplementary Material (ESI) for CrystEngComm.
This journal is © The Royal Society of Chemistry 2014

Supporting Information

Variation of CO_2 Adsorption in Isostructural Cd(II)/Co(II) Based MOFs by Anion Modulation

Udai P. Singh*[a], Shikha Narang[a], Pradip Pachfule[b] and Rahul Banerjee[b]

[a]*Department of Chemistry, Indian Institute of Technology Roorkee, Roorkee-247667, India,*

[b]*Physical/Materials Chemistry Division, CSIR-National Chemical Laboratory, Dr Homi Bhabha Road, Pune-411008, India.*

E-mail: *udaipfcy@iitr.ac.in*

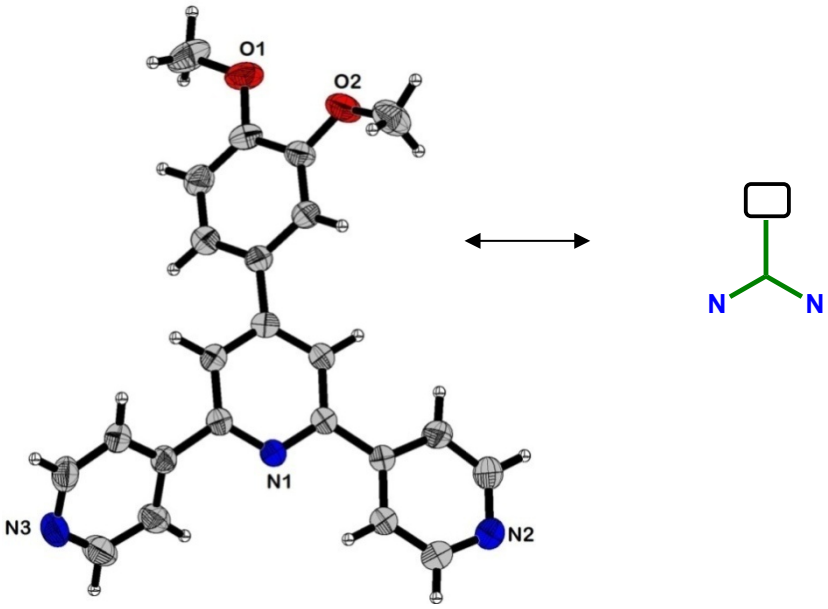

Figure S1. Ortep diagram and simplified form of **dmpt**

Table S1: Crystallographic table for unsqueezed **1-4**

Parameters	1	2	3	4
Emperical formula	$C_{47}H_{39}CdN_8O_{10}Cl_3$	$C_{48}H_{44}Br_2CdN_6O_5S$	$C_{49}H_{45}CdI_2N_7O_5$	$C_{47}H_{39}Cl_5CoN_6O_4$
Formula weight	1094.09	1088.05	1179.06	985.08
Crystal System	Monoclinic	Monoclinic	Monoclinic	Monoclinic
Space Group	*C* 2/*c*	*C* 2/*c*	*C* 2/*c*	*C* 2/*c*
***a*/ Å**	24.6035(5)	24.665(2)	25.6110(7)	24.4845(18)
***b*/ Å**	11.9649(3)	11.9242(11)	11.5667(3)	11.8901(8)
***c*/ Å**	18.4269(4)	17.8777(18)	18.5397(6)	18.1106(13)
***α*/ º**	90	90	90	90
***β*/ º**	114.5710(10)	112.764(4)	114.3450(10)	114.564(4)
***γ* / º**	90	90	90	90
***V* / Å^3**	4933.3(2)	4860.7(8)	5003.7(3)	4795.3(6)
Z	4	4	4	4
***D*$_{calc}$ / g cm^{-3}**	1.520	1.562	1.642	1.416
***F*(000)**	2288.0	2312.0	2432.0	2092.0
μ/mm^{-1}	0.725	2.211	1.728	0.742
θ range/ º	1.82 - 26.42	1.79 - 28.32	1.75 - 26.40	1.83 - 26.42
Reflections collected	41014	16597	31991	36341
Independent reflections	5034	5943	5122	4874
Ranges (h,k,l)	-30< h <30 -14≤ k ≤14 -20≤ l≤ 22	-31≤ h ≤32 -15≤ k ≤15 -23≤ l ≤11	-31≤ h ≤31 -14≤ k ≤14 -23≤ l≤ 23	-20≤ h ≤30 -14≤ k ≤14 -22≤ l ≤18
Complete to 2θ	99.3	98.1	99.8	99.1
GOF(F^2)	1.294	1.339	1.043	1.263
***R*1; w*R*2 [I >2σ(I)]**	0.0732; 0.2639	0.0449; 0.1469	0.0398; 0.1537	0.0969; 0.3121
***R*1; w*R*2 (all data)**	0.0855; 0.2912	0.0567; 0.1627	0.0527; 0.1383	0.1595; 0.3570

[a] $R1 = \sum \| F_o | - | F_c \| / \sum | F_o |$, $wR2 = \{\sum[w(F_o^2 - F_c^2)^2] / \sum w(F_o^2)^2\}^{1/2}$

Section S1. Single crystal X-ray diffraction data collection, structure solution and refinement procedures:

Single crystal data for **1-4** and **dmpt** were collected on performed on a Bruker Kappa Apex four circle-CCD diffractometer using graphite monochromated MoKα radiation (λ = 0.71070 Å) at 100 K and 273 K respectively.

In the reduction of data Lorentz and polarization corrections, empirical absorption corrections were applied.[1] Crystal structures were solved by direct method. Structure solution, refinement and data output were carried out with the SHELXTL program[2-3]. Non-hydrogen atoms were refined anisotropically.

A notable feature of the MOFs reported here is that all MOFs **1-4** are crystallized in same space group *C2/c* with almost same cell parameters and hence results in isostructural MOFs but the solvent molecules in all complexes was highly disordered and was impossible to refine using conventional discrete-atom models; thereby, the share of partial solvent electron densities was rejected by the SQUEEZE program in PLATON[4] and the solvents are tentatively designated based on TGA, elemental analysis as well as the SQUEEZE results i.e. one $CHCl_3$ molecule each in **1** & **4** and one molecule of DMSO & DMF each in **2** & **3** respectively. Notably, the SQUEEZE treated structure is very stable with minimal IUCr checkcif problems, less R factor and goodness of fit. The selected bond lengths are given in Table S2, additionally, MOFs **1-4** also displayed some non – classical C···O and N···O interactions[5] such as C22–H22A···O4, 2.549 Å; C15–H15(Py)···O1, 2.544 Å; C14–H14(Py)···O2, 2.710 Å; N3···O3, 2.901 Å in MOF **1**, C17–H17···Br1, 2.833 Å; C15–H15(Py)···O2, 2.529 Å in MOF **2**, C12–H12···I1, 2.968 Å; C23–H23B···I1, 3.079 Å; C21–H21(Py)···O1, 2.687 Å; C17–H17(Py)···O2, 2.528 Å in MOF **3** and C12–H12···Cl1, 2.771 Å; C23–H23(Py)···O1, 2.623 Å; C17–H17(Py)···O2, 2.564 Å in MOF **4**.

Refine_special_details:

Thermal displacement parameters of some atoms such as C15, C11, O4, N4 and O5 were constrained by using EADP and SIMU for compound **1**. Whereas in compounds **2-4**, only EADP constraint was used on atoms C12 and C11; N3 and C20; N3, C22, O1, C20, C17 and C18 respectively for a better configuration on the structure.

In compound **1-4**, the whole structure is slightly disordered, and that is the reason that the ADPs are elongated. It was deemed that the distortion in the structure is due to static disorder. Though, at low temperature, we achieved a better signal to noise ratio (higher I/sigma), thus leading to much better

agreement factors despite of that, this distortion remains persistent. Similarly, in **1,** the ADPs of nitrate are elongated due to the static disorder.

_Platon_squeeze_details:

According to the TGA analysis and squeeze results, the asymmetric unit of **1** may consist of one distorted chloroform molecule in the pore. But the attempt of modeling the solvent molecule was ineffectual; hence, the electron density was removed by SQUEEZE routine in PLATON to remove the solvent molecules from the pores of **MOF-1**.

```
loop_
 _platon_squeeze_void_nr
 _platon_squeeze_void_average_x
 _platon_squeeze_void_average_y
 _platon_squeeze_void_average_z
 _platon_squeeze_void_volume
 _platon_squeeze_void_count_electrons
 _platon_squeeze_void_content
  1  0.500  0.000  0.047      510      113 ' '
  2  0.000  0.500  0.244      510      113 ' '
```

where, the asymmetric unit of **2** may consist of one distorted DMSO molecule in the pore. But the attempt of modeling the solvent molecule was ineffectual; hence, the electron density was removed by SQUEEZE routine in PLATON to remove the solvent molecules from the pores of **MOF-2**.

```
loop_
 _platon_squeeze_void_nr
 _platon_squeeze_void_average_x
 _platon_squeeze_void_average_y
 _platon_squeeze_void_average_z
 _platon_squeeze_void_volume
 _platon_squeeze_void_count_electrons
 _platon_squeeze_void_content
  1  0.000  0.000 -0.001      578       78 ' '
  2  0.500  0.500  0.244      578       78 ' '
```

The asymmetric unit of **3** may consist of one distorted DMF molecule in the pore. But the attempt of modeling the solvent molecule was ineffectual; hence, the electron density was removed by SQUEEZE routine in PLATON to remove the solvent molecules from the pores of **MOF-3**.

```
loop_
```

```
 _platon_squeeze_void_nr
 _platon_squeeze_void_average_x
 _platon_squeeze_void_average_y
 _platon_squeeze_void_average_z
 _platon_squeeze_void_volume
 _platon_squeeze_void_count_electrons
 _platon_squeeze_void_content
  1  0.000  0.000 -0.008       570       74 ' '
  2  0.500  0.500  0.748       570       74 ' '
```

And the asymmetric unit of **4** may consist of one distorted chloroform molecule in the pore. But the attempt of modeling the solvent molecule was ineffectual; hence, the electron density was removed by SQUEEZE routine in PLATON to remove the solvent molecules from the pores of **MOF-4**.

```
loop_
 _platon_squeeze_void_nr
 _platon_squeeze_void_average_x
 _platon_squeeze_void_average_y
 _platon_squeeze_void_average_z
 _platon_squeeze_void_volume
 _platon_squeeze_void_count_electrons
 _platon_squeeze_void_content
  1  0.500  0.000  0.032       574       253 ' '
  2  1.000  0.500  0.745       574       253 ' '
```

The crystallographic data for unsqueezed MOFs **1-4** have been tabulated in Table S1. The CCDC number for the complexes **1-4** and the ligand, dmpt are CCDC 978705-978709 respectively. Copies of the data can be obtained, free of charge, on application to the CCDC, 12 Union Road, Cambridge CB2 lEZ, U.K. (fax: + 44 (1223) 336 033; e-mail: deposit@ccdc.cam.ac.uk).

Table S2: Bond distances and Angles for **1-4**

$[Cd(dmpt)_2(NO_3)_2]$, **(1)**			
Bond Distances			
Cd1—N3$^{\#1}$	2.375(3)	Cd1—N3$^{\#2}$	2.375(3)
Cd1—N1	2.391(3)	Cd1—N1$^{\#3}$	2.391(3)
Cd1—O3	2.388(4)	Cd1—O3$^{\#3}$	2.388(4)
Bond Angles			
N3$^{\#1}$—Cd1—N3$^{\#2}$	180.00(11)	N3$^{\#1}$—Cd1—N1	93.11(10)
N3$^{\#2}$—Cd1—N1$^{\#3}$	93.11(10)	N3$^{\#1}$—Cd1—N1$^{\#3}$	86.89(10)
N3$^{\#2}$—Cd1—N1	86.89(10)	O3—Cd1—O3$^{\#3}$	180.00(14)
N1—Cd1—O3$^{\#3}$	97.03(11)	N3$^{\#2}$—Cd1—O$^{\#3}$	75.03(13)
N1$^{\#3}$—Cd1—O3$^{\#3}$	82.97(11)	N3$^{\#1}$—Cd1—O3$^{\#3}$	104.97(13)
N1$^{\#3}$—Cd1—O3	97.03(11)	N1—Cd1—O3	82.97(11)
N3$^{\#2}$—Cd1—O3	104.97(13)	N3$^{\#2}$—Cd1—O3	75.03(13)
N1—Cd1—N1$^{\#3}$	180.00(9)		

Symmetry codes for 1: (#1) -0.5+x, 2.5-y, -0.5+z; (#2) 0.5-x, -0.5+y, 0.5-z; (#3) -x, 2-y, -z.

$[Cd(dmpt)_2Br_2]$ **(2)**			
Bond Distances			
Cd1—N3$^{\#1}$	2.399(5)	Cd1—N3	2.399(5)
Cd1—N1$^{\#1}$	2.487(6)	Cd1—N1	2.487(6)
Cd1—Br1$^{\#1}$	2.700(1)	Cd1— Br1	2.700(1)
Bond Angles			
N3$^{\#1}$—Cd1—N3	179.99(17)	N3$^{\#1}$—Cd1—N1$^{\#1}$	87.80(17)
N3—Cd1—N1$^{\#1}$	92.20(17)	N3$^{\#1}$—Cd1—N1	92.20(17)
N3—Cd1—N1	87.80(17)	N1$^{\#1}$—Cd1—N1	180.00(16)

$N3^{\#1}$—Cd1—$Br1^{\#1}$	89.25(12)	N3—Cd1—$Br1^{\#1}$	90.75(12)
$N1^{\#1}$—Cd1—$Br1^{\#1}$	88.86(12)	N1—Cd1—$Br1^{\#1}$	91.14(12)
$N3^{\#1}$—Cd1—Br1	90.75(12)	N3—Cd1—Br1	90.25(12)
$N1^{\#1}$—Cd1—Br1	91.14(12)	N1—Cd1—Br1	88.86(12)

Symmetry codes for **2**: (#1) 1-x, 2-y, -z.

$[Cd(dmpt)_2I_2]$ **(3)**			
Bond Distances			
Cd1—I1	2.880(1)	Cd1—N3	2.426(3)
Cd1—$N3^{\#1}$	2.426(3)	Cd1—$I1^{\#1}$	2.880(1)
Cd1—N3	2.426(3)	Cd1—$I1^{\#1}$	2.880(1)
Cd1—I1	2.880(1)	Cd1—N3	2.426(3)
Cd1—I1	2.880(1)	Cd1—N3	2.426(3)
Cd1—$N3^{\#1}$	2.426(3)	Cd1—$I1^{\#1}$	2.880(1)
Cd1—N1	2.560(3)	Cd1—$N1^{\#1}$	2.560(3)
Bond Angles			
$N3^{\#1}$—Cd1—N3	180.00(12)	$N3^{\#1}$—Cd1—$I1^{\#1}$	88.64(8)
N3#1—Cd1—N1#1	86.27(11)	N1—Cd1—I1#1	91.35(8)
N1—Cd1—I1	88.65(8)	$N3^{\#1}$—Cd1—I1	91.36(8)
$N1^{\#1}$—Cd1—N1	179.99(10)	N3—Cd1—N1	86.27(11)
$N1^{\#1}$—Cd1—I1	91.35(8)	$N3^{\#1}$—Cd1—N1	93.73(11)
$N1^{\#1}$—Cd1—$I1^{\#1}$	88.65(8)	N3—Cd1—$N1^{\#1}$	93.73(11)
I1—Cd1—$I1^{\#1}$	179.98(1)	N3—Cd1—I1	88.64(8)

Symmetry codes for **3**: (#1) 2-x, 1-y, 1-z.

$[Co(dmpt)_2Cl_2]$ **(4)**			
Bond Distances			
Co1—N3	2.203(3)	Co1—N2$^{\#1}$	2.297(6)
Co1—N3$^{\#1}$	2.203(3)	Co1—Cl1	2.430(2)
Co1—N2	2.297(6)	Co1—Cl1$^{\#1}$	2.430(2)
Co1—N3	2.203(3)	Co1—N2$^{\#1}$	2.297(6)
Bond Angles			
N3—Co1—N3$^{\#1}$	179.98(13)	N2$^{\#1}$—Co1—Cl1	92.12(9)
N3—Co1—N2	87.97(12)	N3—Co1—Cl1	89.86(9)
N3$^{\#1}$—Co1—N2$^{\#1}$	87.97(12)	N2—Co1—N2$^{\#1}$	179.99(11)
N3—Co1—N2$^{\#1}$	92.03(12)	N3$^{\#1}$—Co1—Cl1	90.14(9)
N2$^{\#1}$—Co1—Cl1$^{\#1}$	92.12(9)	N2—Co1—Cl1$^{\#1}$	92.12(9)
Cl1—Co1—Cl1$^{\#1}$	180.00(4)	N2—Co1—Cl1	87.88(9)
N3$^{\#1}$—Co1—Cl1$^{\#1}$	89.86(9)	N3$^{\#1}$—Co1—N2	92.03(12)
N3—Co1—Cl1$^{\#1}$	90.14(9)		

Symmetry codes for **4**: (#1) -x, -y, -z.

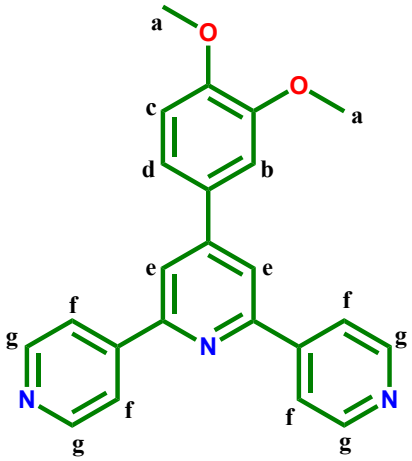

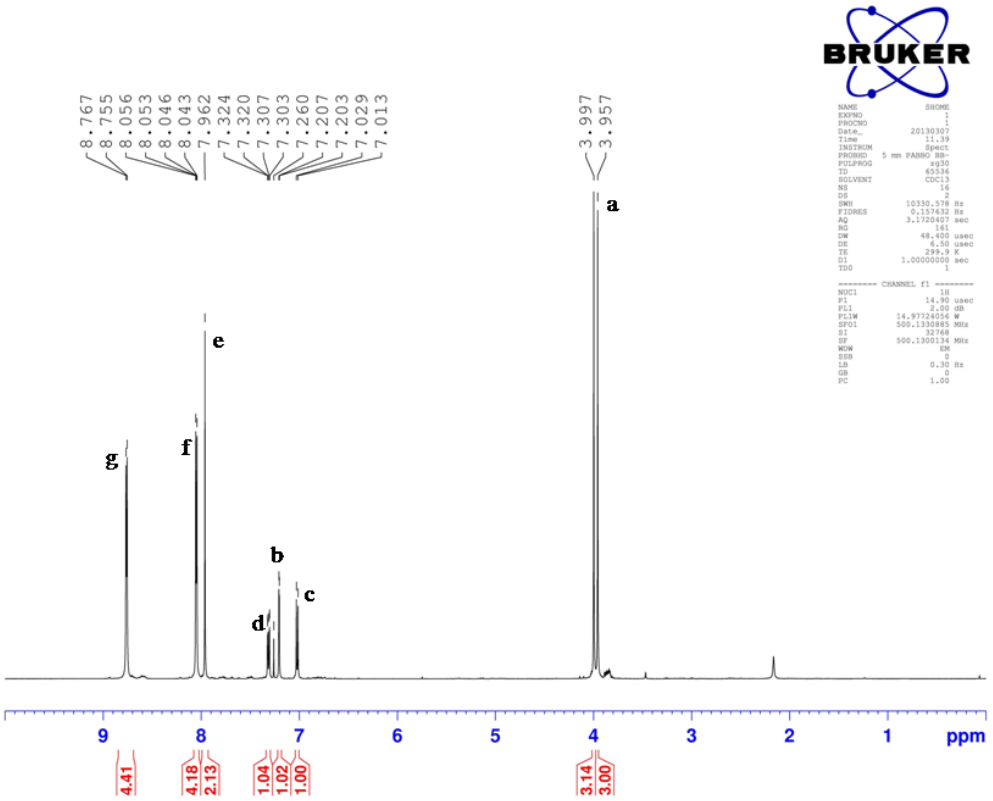

Figure S2. ^{1}H NMR spectra of **dmpt** in $CDCl_3$ as NMR solvent

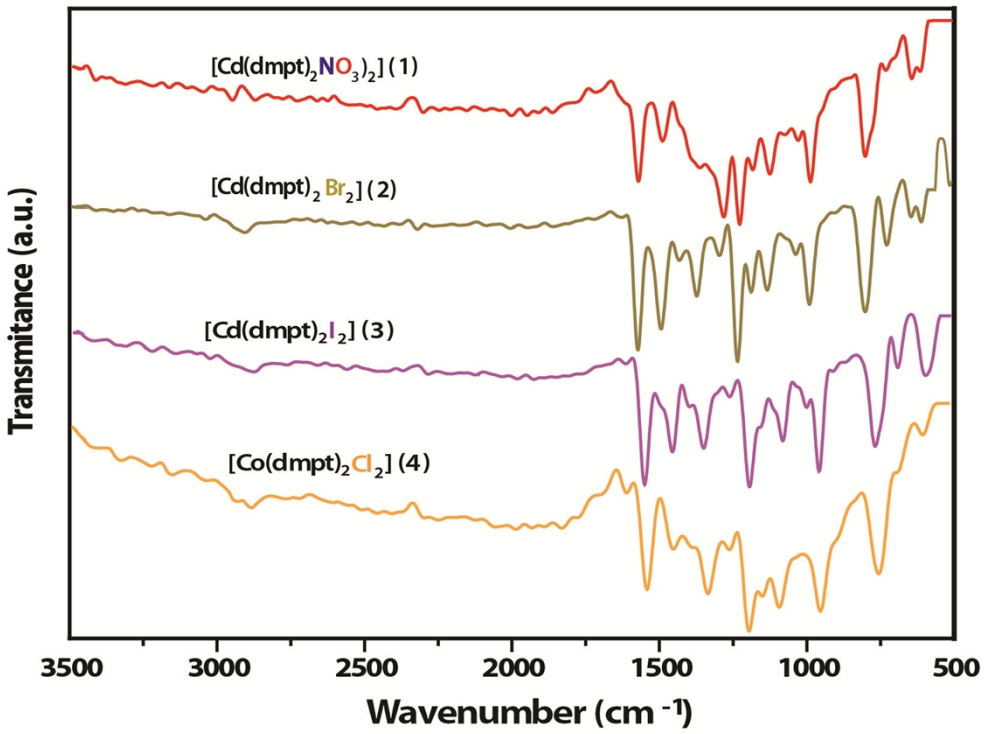

Figure S3. IR spectra for compounds **1-4**

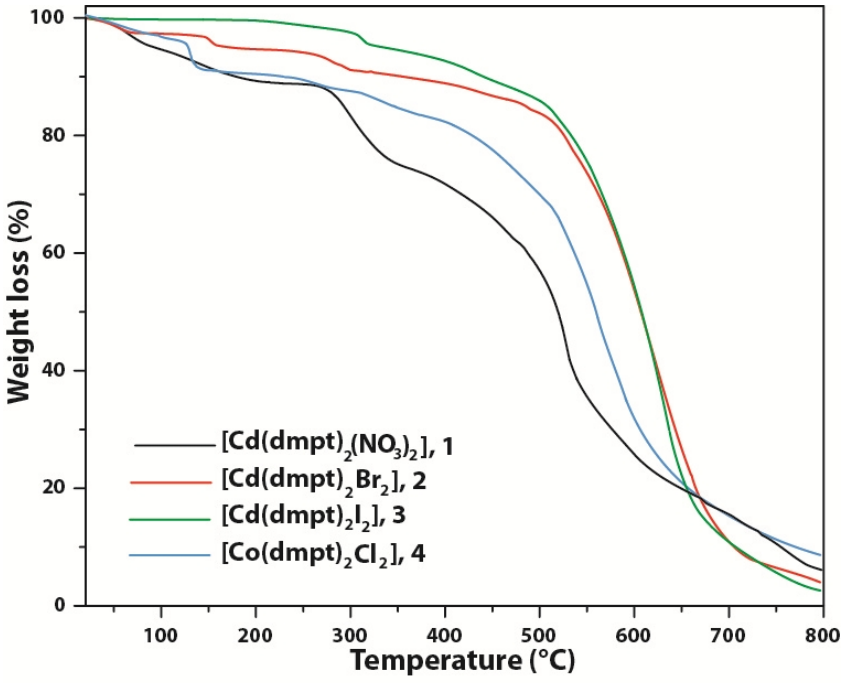

Figure S4. Thermogravimetric analysis curve for **1-4**

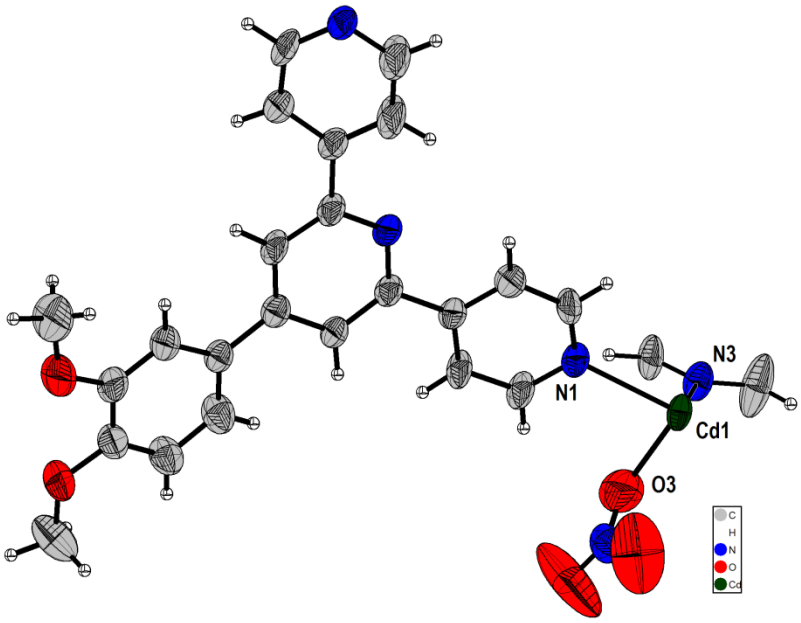

Figure S5: Ortep diagram for **1**

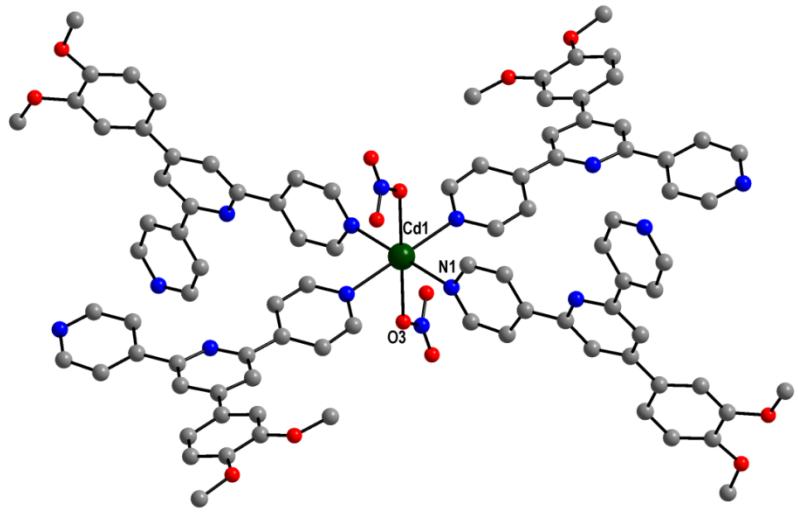

Figure S6. Coordination environment around Cd center in **1**

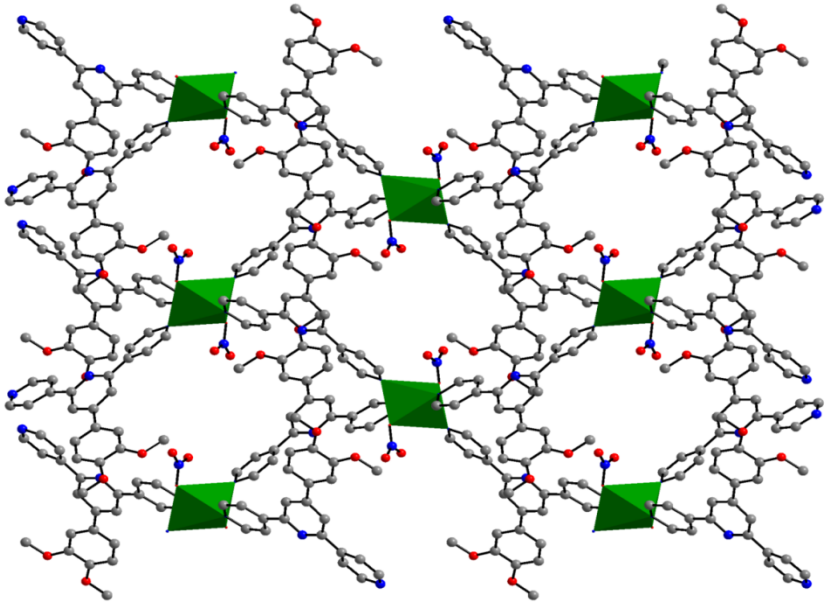

Figure S7. 2D coordination network in **1**

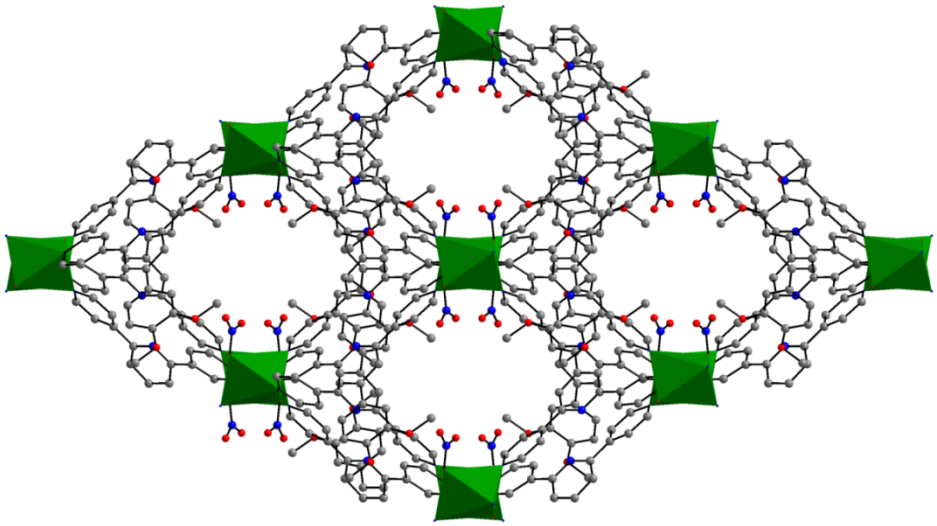

Figure S8. 3D network in **1**

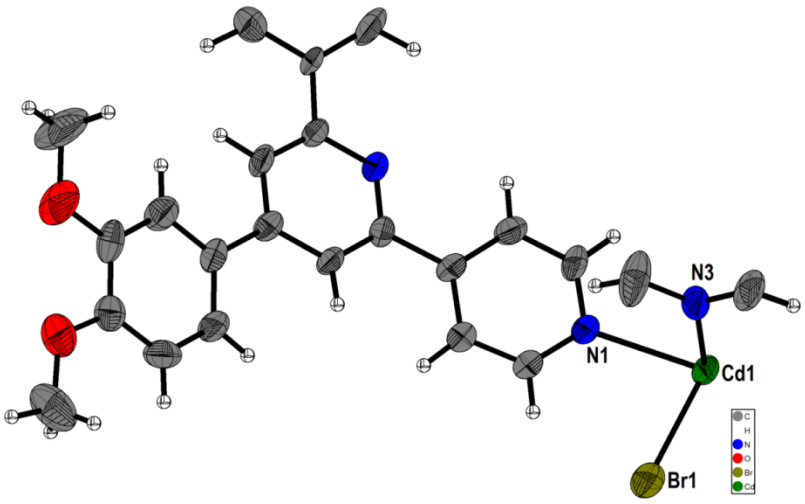

Figure S9. Ortep diagram for **2**

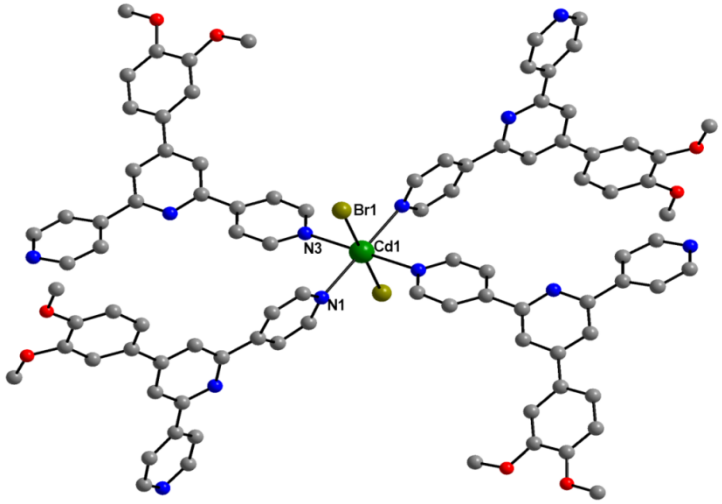

Figure S10. Coordination environment around Cd center in **2**

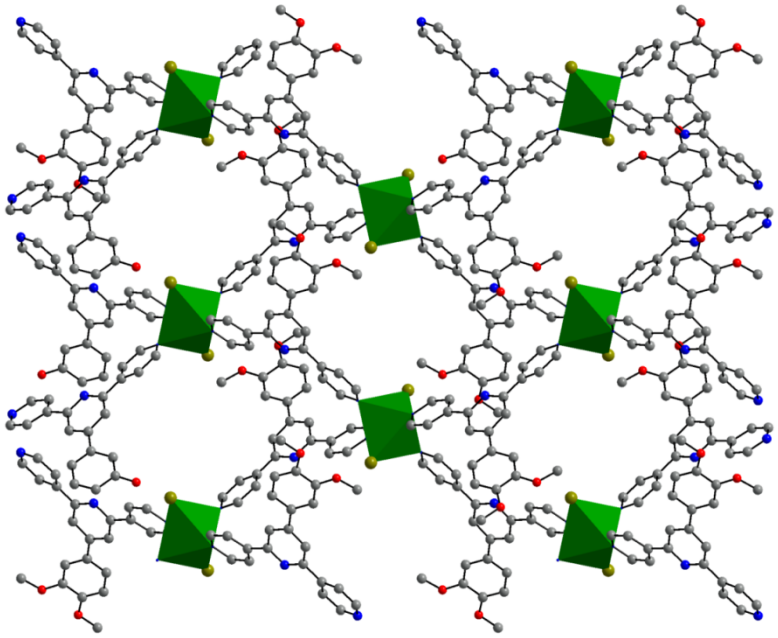

Figure S11. 2D coordination network in **2**

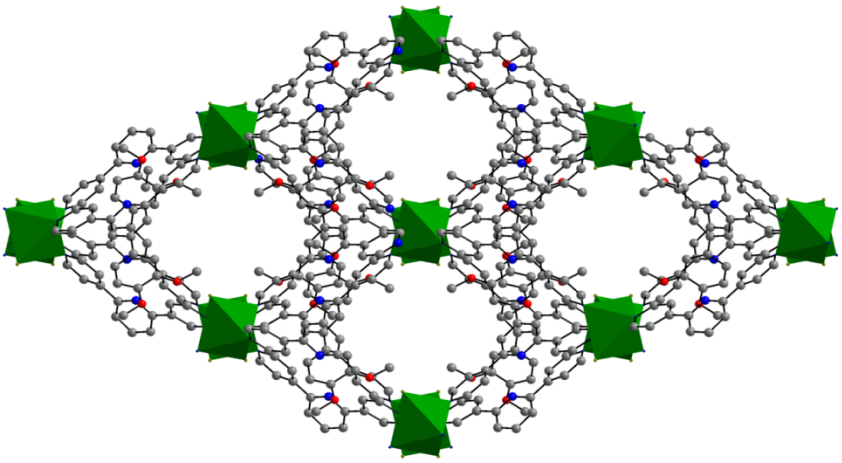

Figure S12. 3D network in **2**

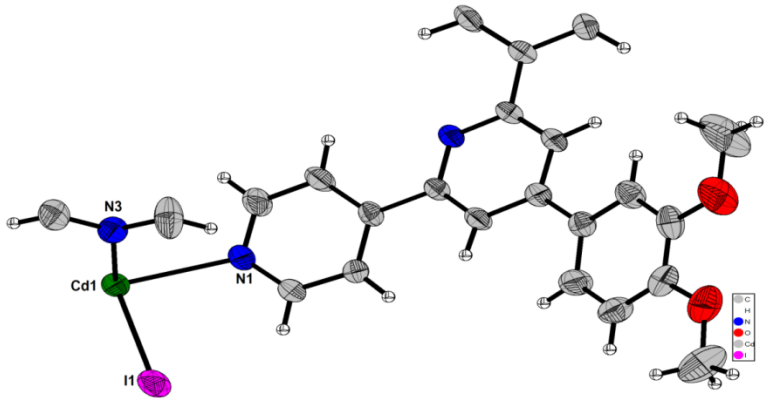

Figure S13. Ortep diagram for **3**

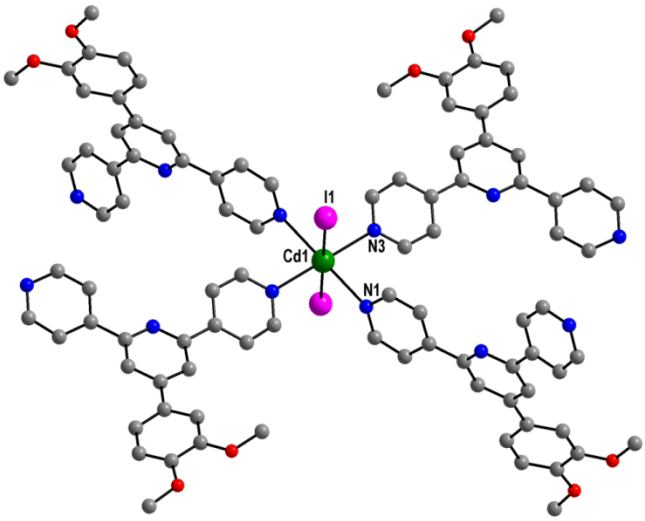

Figure S14. Coordination environment around Cd center in **3**

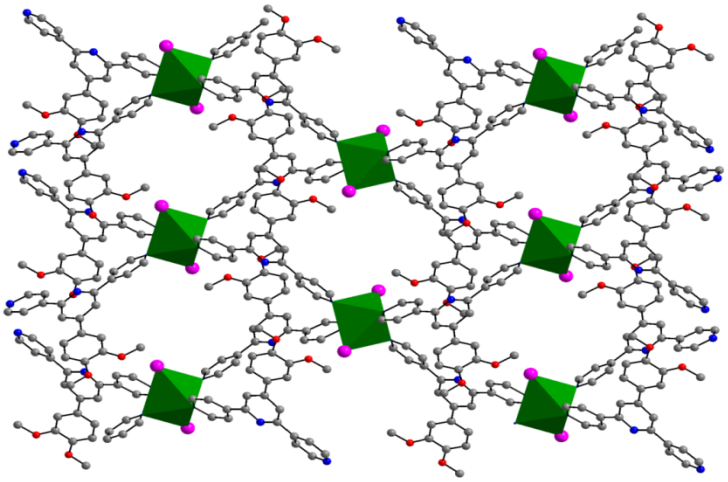

Figure S15. 2D coordination network in **3**

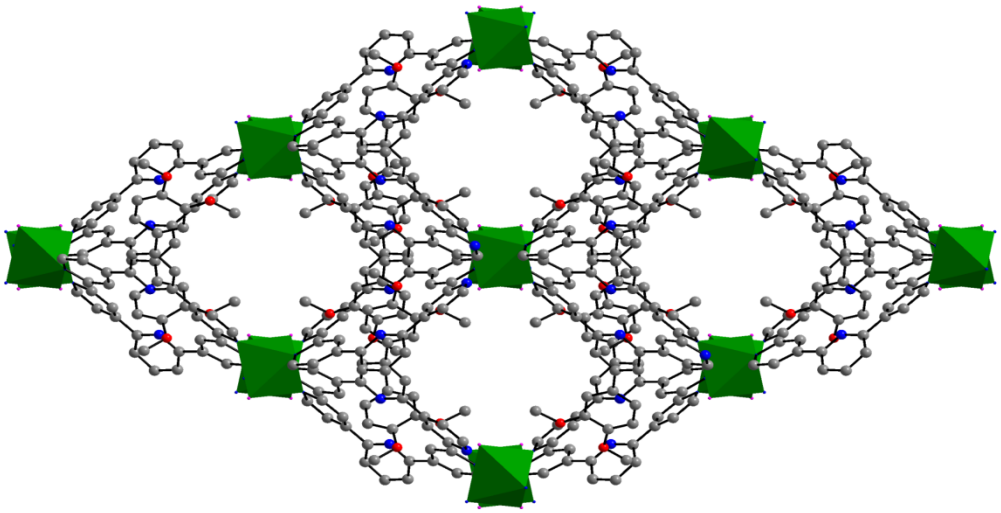

Figure S16. 3D network in **3**

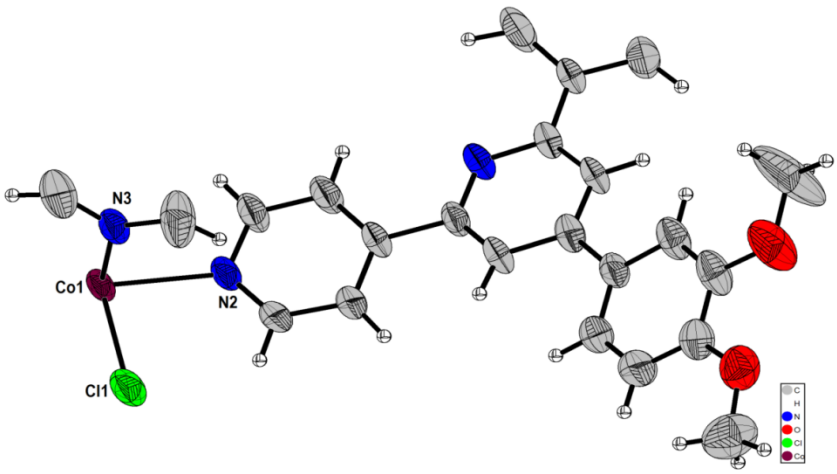

Figure S17. Ortep diagram for **4**

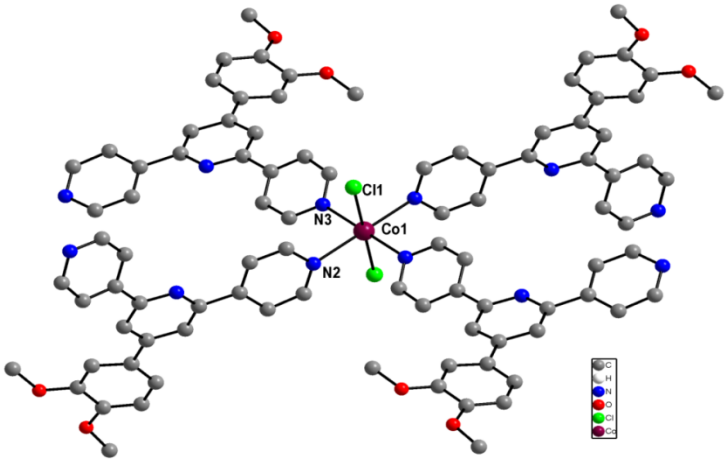

Figure S18. Coordination environment around Co center in **4**

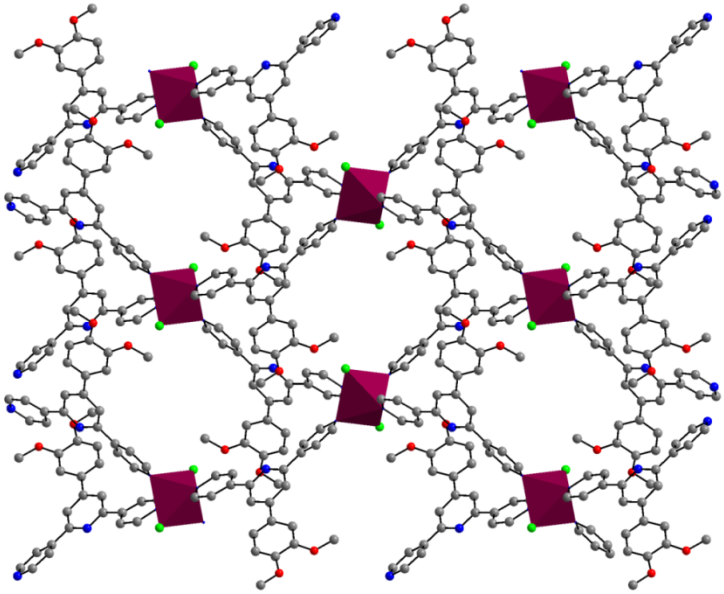

Figure S19. 2D coordination network in **4**

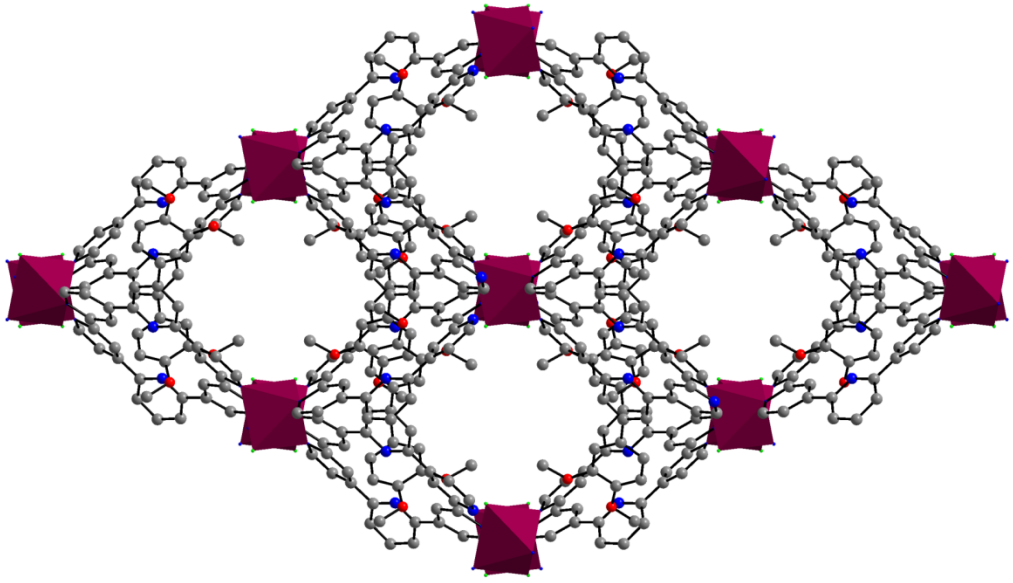

Figure S20. 3D network in **4**

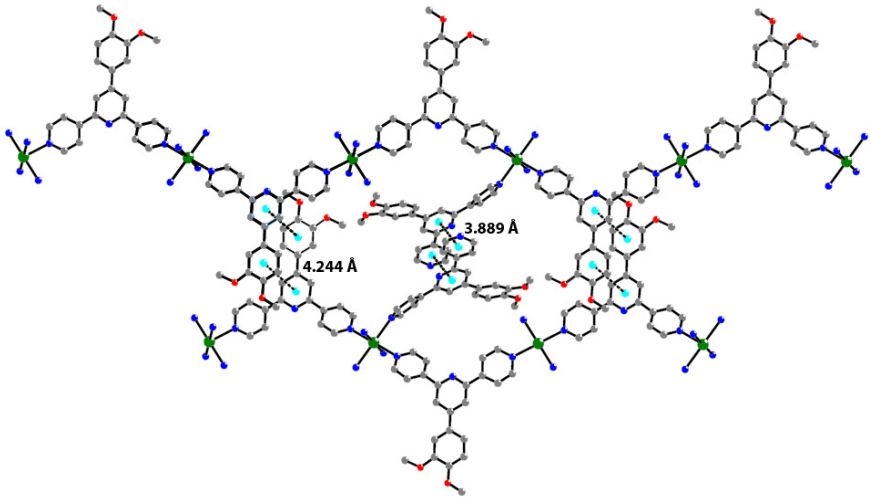

Figure S21. Interlayer π-π stacking between central pyridine rings and between central ring and the pendant ring are 3.889 Å and 4.224 Å respectively.

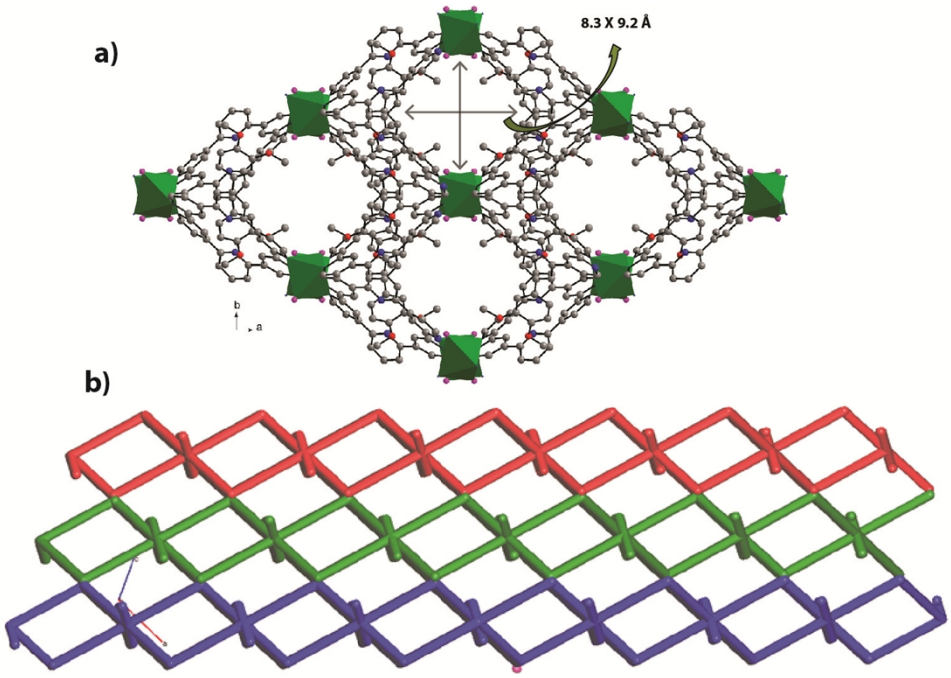

Figure S22. a) View of 1D channel along the crystallographic *c*-axis (b) Side view of 2D networks lying over each other along *ac*-plane, each 2D network is shown by different colour.

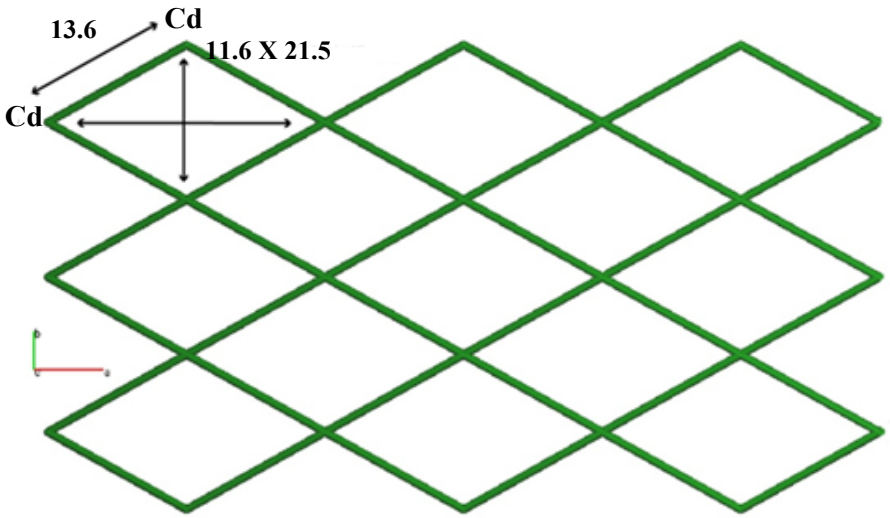

Figure S23. View of Cd-Cd network in 2D framework along *c*-axis presenting the diagonal separation of Cd-Cd (11.6 X 21.5 Å) and Cd-Cd separation bridged by **dmpt** (13.6 Å).

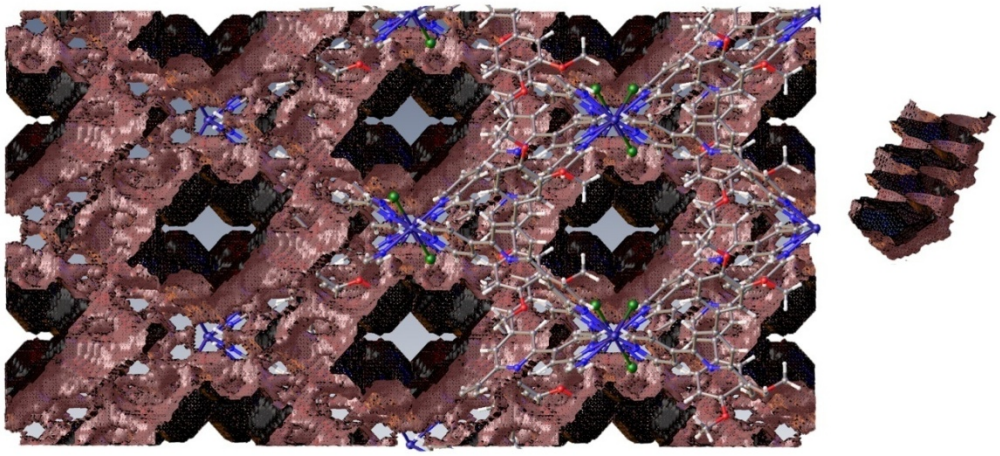

Figure S24: Representation of voids in 3D framework and the cross-section of 1D channel displaying the shape of the channel.

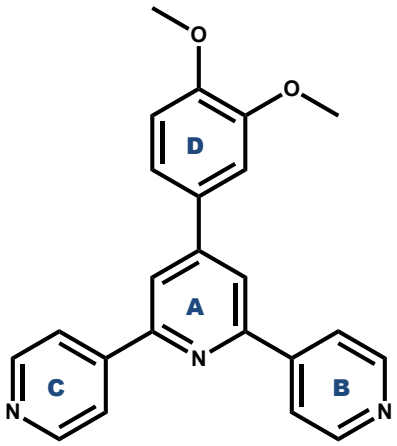

Table S3: Summarizing the torsion angles between the rings of the ligand:

MOFs	Torsion angle between A and B (°)	Torsion angle between A and C (°)	Torsion angle between A and D (°)	Torsion angle between C and B (°)
dmpt	-39.41	-6.36	-37.78	39.68
$[Cd(dmpt)_2(NO_3)_2]$	16.90	-16.95	-15.91	3.65
$[Cd(dmpt)_2Br_2]$	-17.20	21.30	18.96	0.13
$[Cd(dmpt)_2I_2]$	-17.72	21.44	17.18	4.70
$[Co(dmpt)_2Cl_2]$	-20.39	25.93	17.97	6.48

Table S4: Summarizing the pore details of **1-4**.

MOFs	Dimensions of the cavity (Å^2)	Solvent accessible void (Å^3)	Total potential solvent area volume	Packing index (%)	CO_2 Adsorption (cc/g)
$[Cd(dmpt)_2(NO_3)_2]$	6.5 X 6.6	504	4993.3 (20.8%)	58.8	49.5
$[Cd(dmpt)_2Br_2]$	8.1 X 7.4	581	4912.2 (23.6%)	57.0	39.8
$[Cd(dmpt)_2I_2]$	7.0 X 6.9	573	5003.7 (22.9%)	57.2	5.7
$[Co(dmpt)_2Cl_2]$	6.7 X 6.5	573	4795 (24.3%)	57.4	22.6

References:

1. Sheldrick GM, SADABS (1996) University of Göttingen. Göttingen, Germany.
2. Sheldrick GM (1990) *Acta Cryst A* 46:467–473
3. Sheldrick GM SHELXTL-NT 2000 version 6.12, reference manual, University of Göttingen, Göttingen, Germany.
4. Spek, A. L. PLATON99, A Multipurpose Crystallographic Tool; Utrecht University: Utrecht, The Netherlands, 1999.
5. E. Gao, L. Lin, L. Liu, M. Zhu, B. Wang and X. Gao, *Dalton Trans*., 2012, **41**, 11187.